Study on Application of Image Recognition Technology With Deep Learning to Filling Evaluations of Grouted Tendon Ducts

Seiichi Tamura (FUJI P.S CORPORATION, Fukuoka, JAPAN), Hideaki Nakamura (FUJI P.S CORPORATION, Fukuoka, JAPAN), and Masaki Sugie (Dr. Eng, Professor, Yamaguchi University, Yamaguchi, JAPAN)

1. Introduction

The stack imaging of spectral amplitudes based on impact echo (SIBIE) method was developed to make the filling evaluations of grouted tendon ducts easier by using an impact echo method. The SIBIE method is an analysis method that performs spectral analysis of reflected waves and converts the results into a 2D color map.

We examined the application of image recognition technology with deep learning for the purpose of providing technical support for filling evaluations of grouted tendon ducts through the impact echo method using the SIBIE method.

2. Impact echo method using the SIBIE method

2.1 Principles of SIBIE method

An overview of the SIBIE method is shown in Figure 1.

1. A cross-section of the structure is divided into square elements (10 mm by 10 mm).
2. It is assumed that the elastic wave is input at the excitation point reflected at any point and reaches the measurement points 1 and 2 through the shortest propagation distance. The resonant frequency f_R (Hz) generated by reflection is calculated using Eq. (1)., the elastic wave speed is Cp (m/sec), and the shortest propagation distance (m) is R (sensor 1: R=r1+r2, sensor 2: R=r1+r3).

$$f_R = Cp/R \qquad (1)$$

3. A relative amplitude value y_R is calculated for each node divided into elements.
4. The relative amplitude value y_R (sum of sensors 1 and 2) of each node is determined from the frequency spectrum obtained by FFT.
5. A 2D color map is created, color-coded into five colors according to the size of y_R.

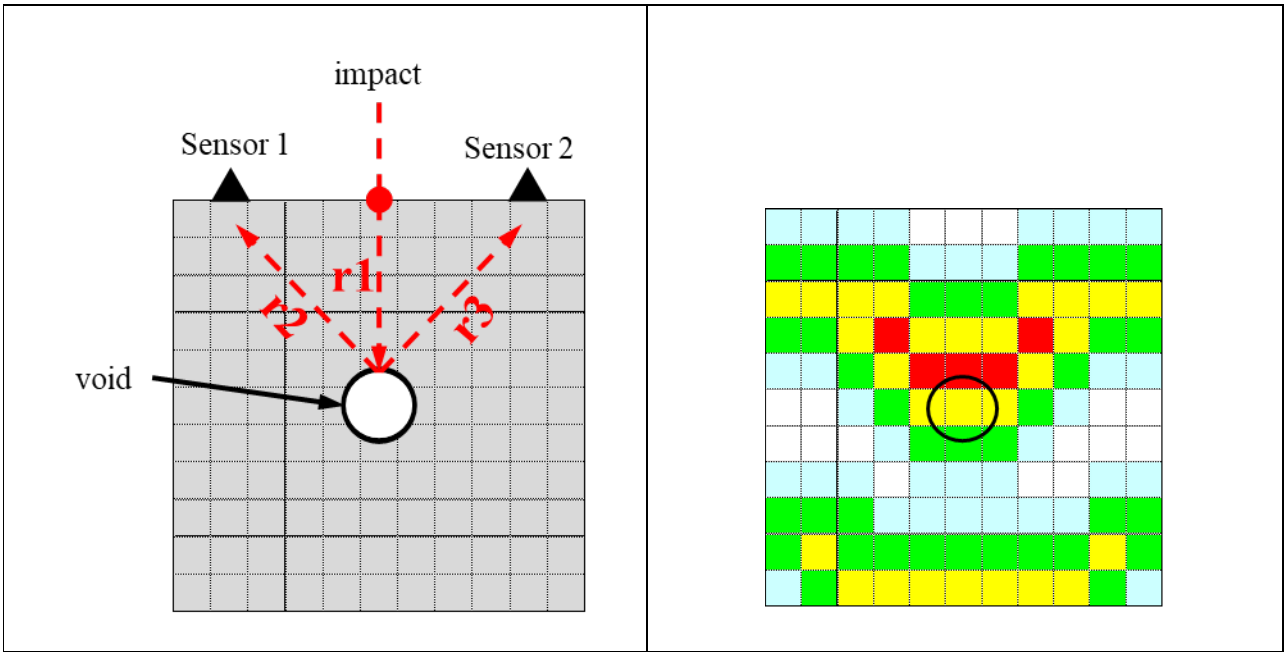

modeling	2D color map

Figure 1. SIBIE method

2.2 Filling evaluations of grouted tendon ducts

The condition of the grouting evaluations using the 2D color maps obtained with the SIBIE method is determined by the position of the part with a large amplitude value (red area) (Figure 2).

Evaluation	Grouted	Ungrouted	Possibility of being un-grouted	Difficult to determine
Position of red area	On other side	Tendon duct circumference	Tendon duct interior	Other
2D map	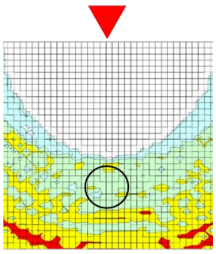	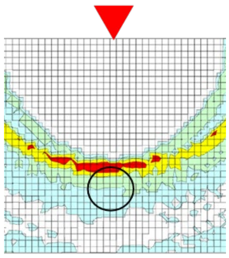	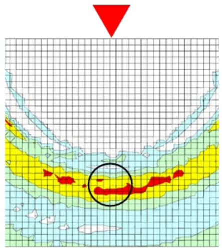	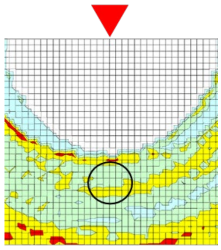
▼: Impact ○: Tendon duct Bottom side is the other side				
Relative amplitude value y_R		Larger ... Smaller		

Figure 2. Filling evaluations of grouted tendon ducts

3. Preparation, etc.

3.1 Data set

Data before and after the filling of grouted tendon ducts was collected from the main cables of two post-tension box-girder bridges and five post-tension segment T-girder bridges.

The breakdown of the collected data is shown in Table 1. The waveform data collected totaled 3,775 pieces before the filling of grouted tendon ducts and 3,795 pieces after the filling of grouted tendon ducts, for a grand total of 7,570 pieces of data.

3.2 Deep learning

Deep learning used convolutional neural networks (CNN), which are used in various fields. As the collected waveform data is characterized by two classifications, before the filling of grouted tendon ducts and after the filling of grouted tendon ducts, and because it is a relatively simple image with a fixed size and color, the network model of the CNN was the network model of VGG16 (trained on ImageNet), which

Table 1. Data set

Tendon duct depth	Grouted tendon duct		Tendon duct depth	Grouted tendon duct	
:L	Before filling	After filling	:L	Before filling	After filling
(mm)	(pieces)	(pieces)	(mm)	(pieces)	(pieces)
110–120	820	830	230–240	200	200
130–140	180	180	250–260	280	280
140–150	90	90	260–270	60	60
160–170	20	20	270–280	195	200
170–180	355	355	290–300	15	15
180–190	60	60	300–310	245	250
190–200	20	20	310–320	390	390
210–220	280	280	340–360	505	505
220–230	40	40	420–440	20	20
			Sub Total	**3,775**	**3,795**
			Total		**7,570**

is easy to handle (Figure 3). Data augmentation and fine-tuning were performed to improve the generalization performance as much as possible.

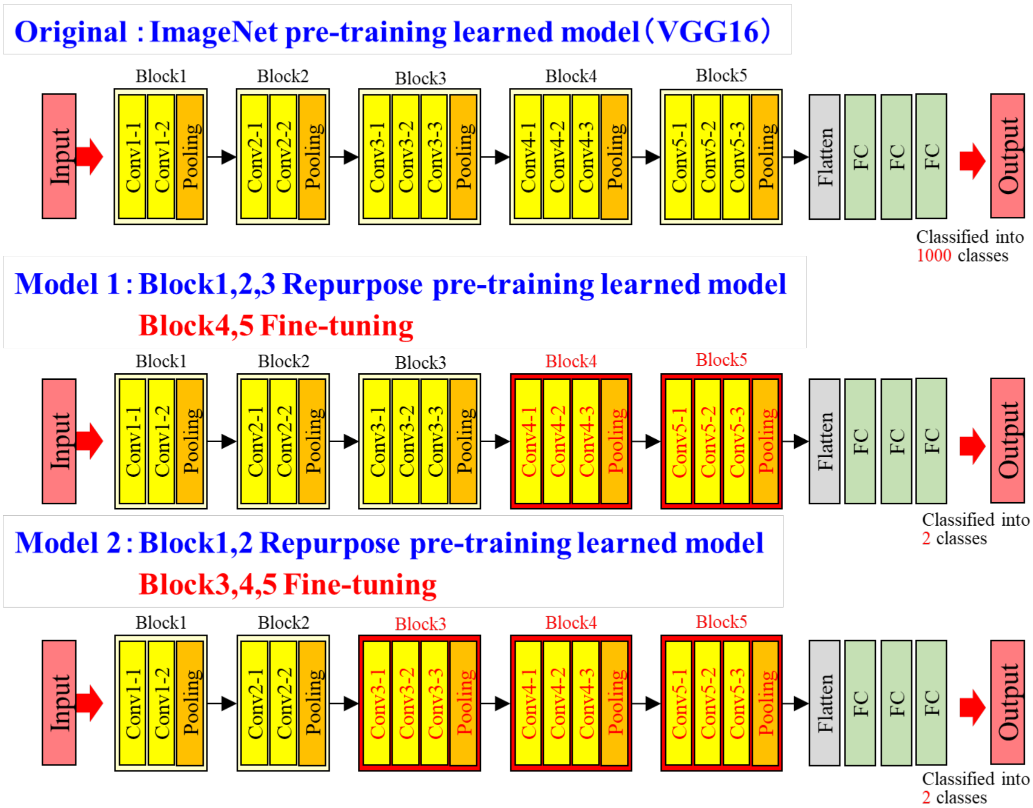

Figure 3 VGG16

3.3 Data set partitioning and 5-Fold Cross-Validation

Data set partitioning and the 5-Fold Cross-Validation are shown in Figure 4.

1. The data set for before and after the filling of grouted tendon ducts is divided into the training data used for 5-fold cross-validation (80% of the total) and the test data used to confirm the generalization performance (the remaining 20%) using random numbers.
2. The training data in 1 is divided into five equal parts (G1–G5), of which four are training data and one is validation data. Five types of training data were created with different validation data.

3.4 Data augmentation

Common methods of data augmentation include brightness modification, scaling, rotation, mirror image reversal, and noise addition. 2D color maps obtained with the SIBIE method can only be mirrored horizontally in data augmentation. Due to the lack of data augmentation

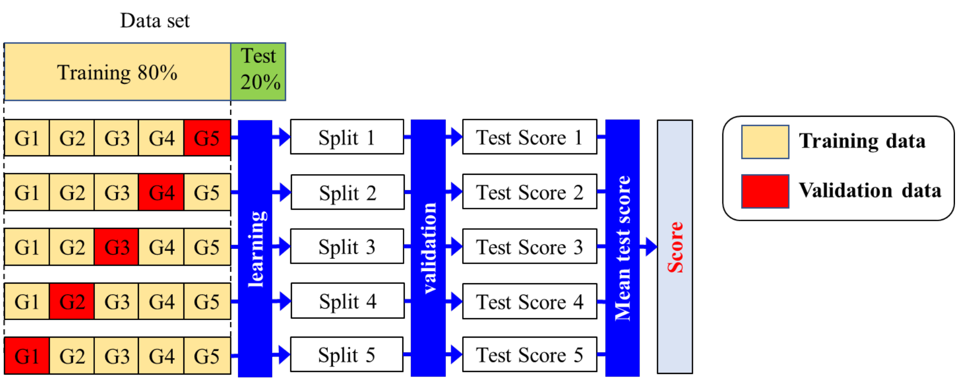

Figure 4. 5-Fold Cross-Validation

methods, the data count used in deep learning is insufficient. Therefore, we developed a new way to expand data augmentation options.

Concrete is a heterogeneous composite material composed of water, air, cement, and aggregate. Data augmentation was performed by taking advantage of the properties of concrete (Figure 5).

The method of data augmentation is as follows.

1. An arbitrary elastic wave speed is set for each divided cell.

The elastic wave speed is assumed to be a normal random number, and the standard deviation is changed by trial and error and set as 200 m/sec^2.

2. Eq. (2) and Eq. (3) are used to calculate the resonant frequency: f_R (Hz).

$$f_R = 1 / \Sigma T \tag{2}$$

$$\Sigma T = Lp1/Cp3 + Lp2/Cp2 + Lp3/Cp5 + Lp4/Cp4 + Lp5/Cp4 + Lp6/Cp1 \tag{3}$$

ΣT: Time from the excitation point to pass through any node and reach the measurement point

Lp: The distance that the elastic wave passed through the cell

Cp: Elastic wave speed

The frequencies of all nodes are calculated from Eq. (2) and Eq. (3), and the amplitude value is obtained from the frequency spectrum.

3. A 2D color map is created using the SIBIE method.

The condition required for the 2D color map created through data augmentation must be the same filling evaluation result of a grouted tendon duct as the original data.

Figure 6 shows 2D color maps created through data augmentation to change the elastic wave speed. By changing the elastic wave speed for each cell, the filling evaluation of the grouted tendon duct does not change but a different 2D color map can be created.

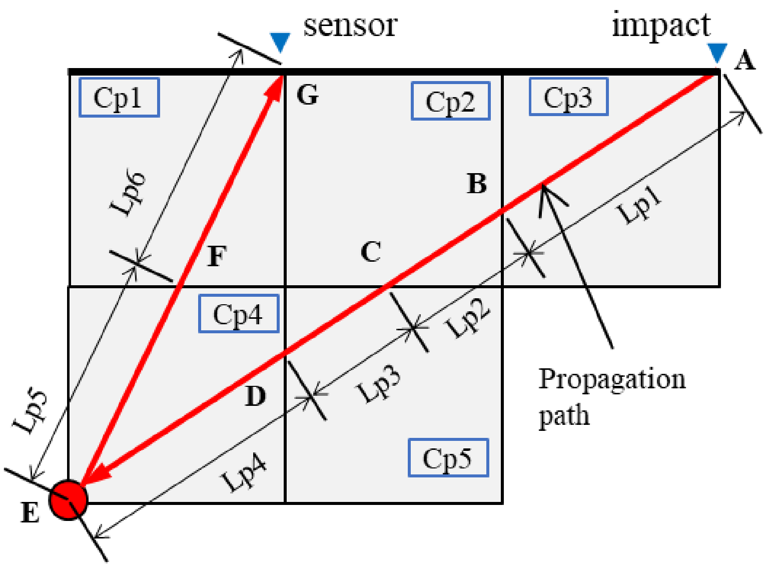

Cp1～Cp5 ：Elastic wave speed

Lp1～Lp6：propagation distance

A～G ：The intersection of the propagation path with the perimeter of the cell

Figure 5. Modeling the propagation of acoustic waves inside concrete

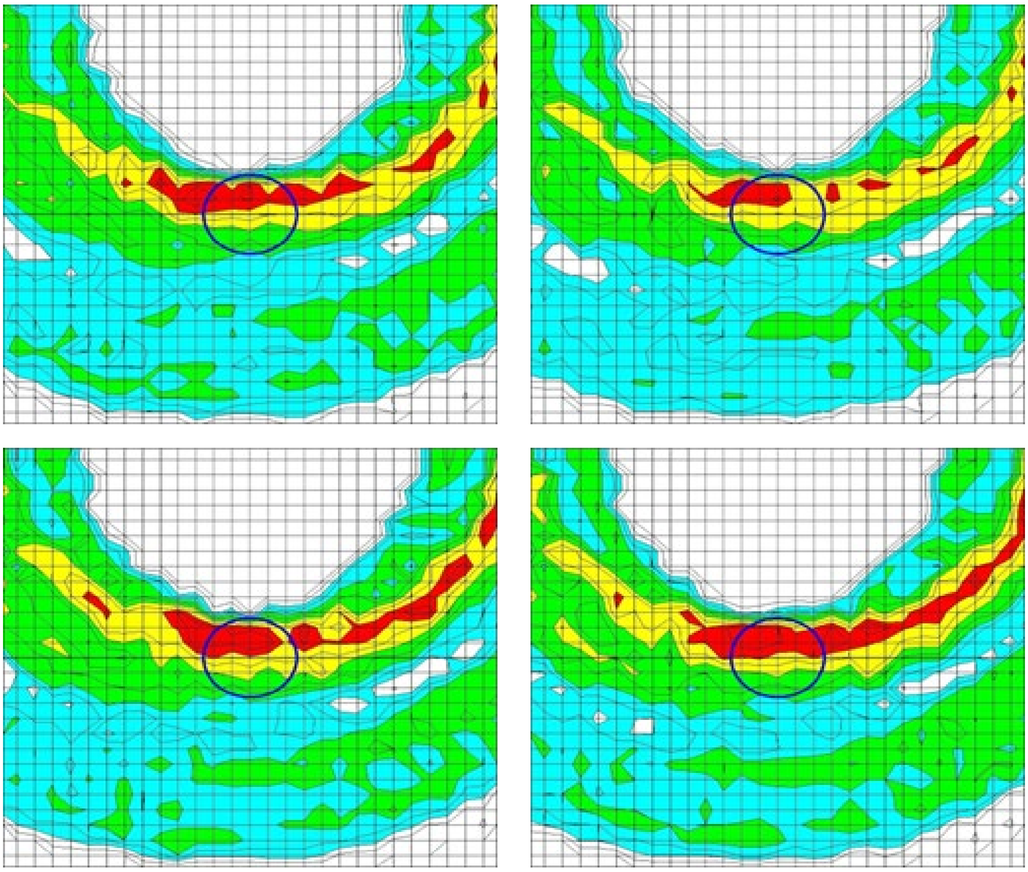

Figure 6. 2D color maps created through data augmentation

4. Examination of applicability to filling evaluations of grouted tendon ducts

Using the data set in Table 1, we confirmed the effect of the difference in the combination of data augmentation and fine-tuning, as well as the difference in the tendon duct depth and the number of pieces of training data, on the accuracy rate of filling evaluations of grouted tendon ducts.

4.1 Changes in accuracy rate due to differences between data augmentation and fine-tuning

Table 2 shows the results of verification using the learning content and test data. Three cases of training data were created by combining different data augmentation methods and the range of fine-tuning. In all three cases, horizontal mirror-image inversion was performed for data augmentation. In case 3, data augmentation that changes the elastic wave speed has been added, and the number of pieces of training data was increased by 20 times. For fine-tuning, training data was created by readjusting Blocks 4 and 5 and Blocks 3, 4, and 5 in Figure 5.

In the case of Case 1, the accuracy was 76.7%. By expanding the range of fine-tuning as in Case 2, accuracy was improved by about 2% compared to Case 1 from Table 2. The reason for the improvement in accuracy is that the 2D color map is a relatively simple image with limited features compared to photographs, etc., and the features were extracted from the initial stage close to the input layer of the CNN.

In Case 3, the generalization performance was improved by training with the 2D color map created through data augmentation, and the accuracy rate was the highest among the three cases.

4.2 Effects of differences in tendon duct depth and data count

Table 3 shows the verification results when the training content is changed by tendon duct depth, and Figure 7 shows the relationship between tendon duct depth and the accuracy rate. Case 0 in Table 3 is the same as Case 3 in the previous section. The accuracy rate decreased as the tendon duct depth increased from Figure 7. This is because when elastic waves propagate, the deeper the tendon duct, the more it is affected by the medium (concrete), and the 2D color map is complicated by the influence of the medium. There was no relationship between the data count and the percentage of correct answers.

Table 2. Verification results with test data

	Deep learning				Verification results with test data								
	Data augmentation		Fine-tuning		Actual (before filling of grouted tendon duct)				Actual (after filling of grouted tendon duct)				Mean accuracy
	Mirror image reversal (horizontal)	Elastic wave speed change	Block 3, 4, 5	Block 4, 5	Correct	Incorrect	Total	Accuracy	Correct	Incorrect	Total	Accuracy	
Unit	–	–	–	–	pieces			%	pieces			%	%
Case 1	●	–	–	●	602	150	752	80.1	526	192	718	73.3	76.7
Case 2	●	–	●	–	592	160	752	78.7	564	154	718	78.6	78.6
Case 3	●	●	–	●	634	118	752	84.3	599	119	718	83.4	83.9

4.3 Calculation of confusion matrix and evaluation index

If the PC grout is predicted to be "after the filling of the grouted tendon duct" even though it is "before the filling of the grouted tendon duct," it is evaluated that the ungrouted duct has been overlooked (dangerous evaluation) in the filling investigation of grouted tendon ducts, which is intended to protect PC strands. Therefore, we calculated a confusion matrix and an evaluation index used as an index to measure the performance of a binary classification machine learning model and confirmed the probability of making dangerous evaluations.

The confusion matrix of Cases 0 –7 in Table 3 is shown in Table 4, and the calculation results of the confusion matrix are shown in Table 5. From Table 5, the recall rate (the probability that the actual measurement correctly predicted before PC grout filling) decreased as the duct position deepened and decreased to 0.72. To utilize image recognition technology based on deep learning in filling evaluations of grouted tendon ducts, it is necessary to further increase the recall rate.

Table 3. Accuracy rate when changing the sheath depth

	Total	Deep learning			Verification results with test data								
		Tendon duct depth			Actual condition (before filling grouted tendon duct)				Actual condition (after filling grouted tendon duct)				Mean accuracy
		Median	Lower Limit	Upper limit	Correct	Incorrect	Total	Accuracy	Correct	Incorrect	Total	Accuracy	
unit	pieces	mm	mm	mm	pieces	pieces	pieces	%	pieces	pieces	pieces	%	%
Case0	7,570	270	110	430	634	118	752	84.3	599	119	718	83.4	83.9
Case1	2,230	140	110	170	191	22	213	89.7	210	11	221	95.0	92.3
Case2	1,090	170	140	200	93	8	101	92.1	99	15	114	86.8	89.5
Case3	1,510	200	170	230	146	16	162	90.1	132	18	150	88.0	89.1
Case4	1,600	230	200	260	118	37	155	76.1	127	20	147	86.4	81.3
Case5	1,475	260	230	290	104	41	145	71.7	131	32	163	80.4	76.0
Case6	1,820	290	260	320	137	40	177	77.4	139	40	179	77.7	77.5
Case7	2,355	360	290	430	169	64	233	72.5	190	54	244	77.9	75.2

5. Visualization of areas of interest with Score-CAM

When performing a filling evaluation of a grouted tendon duct, the person pays attention to the large amplitude around the duct, inside, and on the opposite side according to the properties of the elastic wave and makes an evaluation with reference to the evaluation criteria in Figure 3. CNN, like people, needs to perform the evaluation according to the nature of elastic waves. However, we do not know where the CNN focuses on the 2D color map based on the results of Tables 3–5 (black box problem). Therefore, we used Score-CAM to visualize the focus areas that serve as the basis for the evaluation. Score-CAM is a mapping method that allows us to obtain visual information by visualizing the

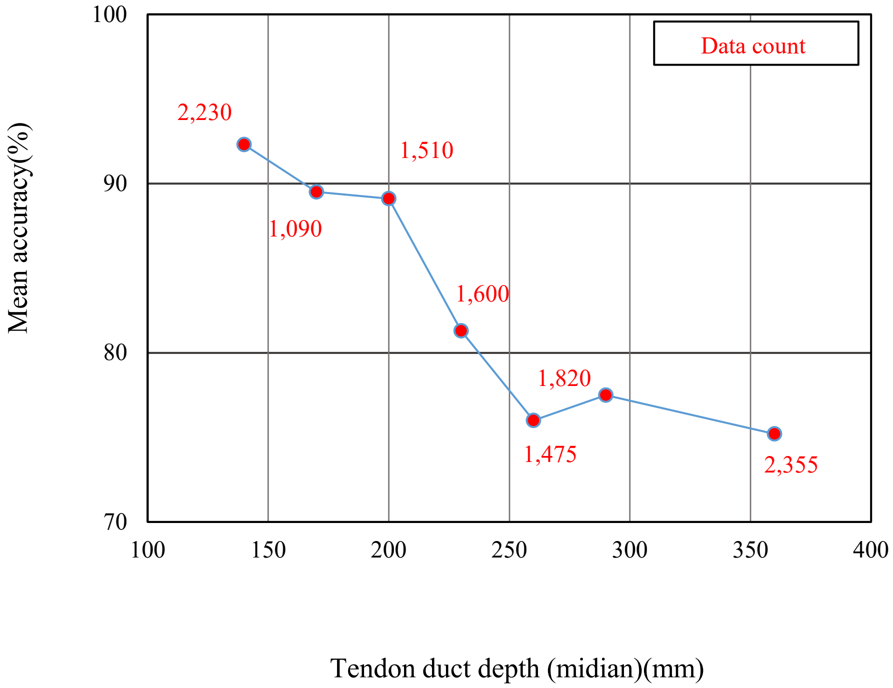

Figure 7. Relationship between tendon duct depth and accuracy rate

part of the CNN that we are focusing on like a heat map.

The results of visualizing the focus areas with Score-CAM are shown in Figure 8. The reason for selecting the 2D color map in Case 1 of Table 4 is that the accuracy rate is the highest in Table 5, and there is a high possibility that the basis for the false evaluations in Fig. 8 (a), (c), and (d) were in the same focus areas as humans. However, in Fig. 8 (b), there were not only the same focus areas as humans but also focus areas in the upper right and lower left regions, which are not focus areas when people conduct evaluations. In addition, the focus areas in Fig.

Table 4. Confusion matrix

Case 0		Predicted condition	
		Before	After
Actual condition	Before	634	118
	After	119	599

Case 4		Predicted condition	
		Before	After
Actual condition	Before	118	37
	After	20	127

Case 1		Predicted condition	
		Before	After
Actual condition	Before	191	22
	After	11	210

Case 5		Predicted condition	
		Before	After
Actual condition	Before	104	41
	After	32	131

Case 2		Predicted condition	
		Before	After
Actual condition	Before	93	8
	After	15	99

Case 6		Predicted condition	
		Before	After
Actual condition	Before	137	40
	After	40	139

Case 3		Predicted condition	
		Before	After
Actual condition	Before	146	16
	After	18	132

Case 7		Predicted condition	
		Before	After
Actual condition	Before	169	64
	After	54	190

Before: Before filling of grouted tendon duct

After: After filling of grouted tendon duct

Table 5. Calculation

	Accuracy	Precision	Recall
Case 0	0.84	0.84	0.84
Case 1	0.90	0.95	0.90
Case 2	0.92	0.86	0.92
Case 3	0.90	0.89	0.90
Case 4	0.77	0.86	0.76
Case 5	0.74	0.76	0.72
Case 6	0.78	0.77	0.77
Case 7	0.74	0.76	0.73

Calculation formula

Accuracy = (TP+TN)/(TP+FP+TN+FN)

Precision= TP/(TP+FP)

Recall = TP/(TP+FN)

Case		Predicted condition	
		Before	After
Actual condition	Before	TP	FN
	After	FP	TN

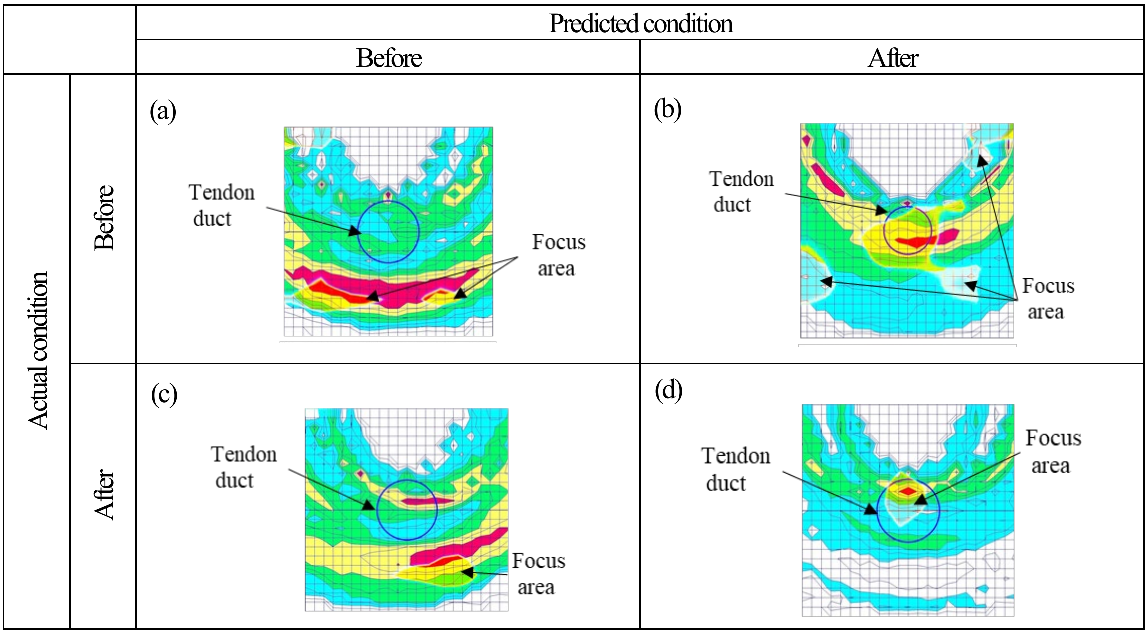

Figure 8. Visualization of areas of interest with Score-CAM

8 (b) that differ from people and the focus area in Figure 8 (c) shared with people were false positives. It was found that the focus areas are sometimes different from those of people, and that there is no clear relationship between the focus areas and false positives.

6. Conclusion

In this paper, we applied deep learning to the measurement results (2D color maps) obtained with the impact echo method using the SIBIE method. As a result, the accuracy rate is as low as 92.3% at the maximum. There are also differences depending on the tendon duct depth, leading us to believe that it will be difficult to put it to practical use at present. However, considering that deep learning can be applied, and that the accuracy rate was improved through data augmentation, we feel that there is a possibility of aiding filling evaluations of grouted tendon ducts. For practical application, it will be necessary to increase the accuracy rate and recall rate while checking the evaluation results of the CNN and the focus areas. The specific tasks are as follows.

1. Data should be collected under different conditions, such as the depth of the duct, the diameter, and the thickness of the member. This data can then be used to create training data.

2. The 2D color maps should be improved so that detailed features of amplitude values can be expressed (e.g.: 2D color maps, which are currently color-coded into five levels according to the magnitude of the amplitude value, should be color-coded into ten levels).

When image recognition technology based on deep learning is applied to improve the efficiency of human tasks, we will need to consider how to ensure sufficient training data and new ways to augment data. We hope that the method introduced in this article will be helpful when doing so.